1 **Stimulus-Locked Responses on Human Upper Limb Muscles and Corrective Reaches are**
2 **Preferentially Evoked by Low Spatial Frequencies**
3
4 Abbreviated title: Low spatial frequencies evoke fast visuomotor responses
5

6 Rebecca A. Kozak[1,5], Philipp Kreyenmeier[2], Chao Gu[3,5], Kevin Johnston[4,5], Brian D.
7 Corneil[1,3,4,5]
8
9 [1]Graduate Program in Neuroscience, Western University, London, On, Canada, N6A 5B7
10 [2]Graduate Program in Neuro-cognitive Psychology, Ludwig Maximilian University of Munich,
11 Munich, Germany, 80539
12 [3]Department of Psychology, Western University, London, Ontario, Canada, N6A 5B7
13 [4]Department of Physiology and Pharmacology, Western University, London, Ontario, Canada,
14 N6A 5B7
15 [5]Robarts Research Institute, 1151 Richmond St. N, London, Ontario, Canada, N6A 5B7
16

17 **Correspondence should be addressed to:**
18 Dr. Brian D. Corneil
19 Robarts Research Institute
20 1151 Richmond St N
21 London, ON, Canada N6A 5B7
22 Phone: (519) 663-5777, ext 24132
23 E-mail: bcorneil@uwo.ca
24
25 **Key words:** Visually-guided reaching, electromyography, online correction, spatial frequency
26
27 Number of pages: 35
28 Number of figures: 10
29 Number of works for Abstract: 236, Introduction: 565, and Discussion: 1491
30
31 Conflicts of interest: The authors declare no competing financial interests
32

39

40

41

42

43    **Abstract (236/250)**

44    In situations requiring immediate action, humans can generate visually-guided responses at

45    remarkably short latencies. Here, to better understand the visual attributes that best evoke such

46    rapid responses, we recorded upper limb muscle activity while participants performed visually-

47    guided reaches towards Gabor patches composed of differing spatial frequencies. We studied

48    reaches initiated from a stable posture (experiment 1, a static condition), or during on-line reach

49    corrections to an abruptly displaced target (experiment 2, a dynamic condition). In both

50    experiments, we detail the latency and prevalence of stimulus-locked responses (SLRs), which

51    are brief bursts of EMG activity that are time-locked to target presentation rather than movement

52    onset. SLRs represent the first wave of EMG recruitment influenced by target presentation, and

53    enable quantification of rapid visuomotor transformations. In both experiments, reach targets

54    composed of low spatial frequencies elicited the shortest latency and most prevalent SLRs, with

55    SLR latency increasing and SLR prevalence decreasing for reach targets composed of

56    progressively higher spatial frequencies. SLRs could be evoked in either the static or dynamic

57    condition, and when present in experiment 2, were associated with shorter latency and larger

58    magnitude corrections. Furthermore, SLRs evolved at shorter latencies (~20 ms) when the arm

59    was already in motion. These results demonstrate that stimuli composed of low spatial

60    frequencies preferentially evoke the most rapid visuomotor responses which, in the context of

61    rapidly correcting an on-going reaching movement, are associated with earlier and larger on-line

62    reach corrections.

63

64

65

66    **Significance Statement (95/120 words)**

67    Humans have a remarkable capacity to respond quickly to changes in our visual environment.

68    Although our visual world is composed of a range of spatial frequencies, surprisingly little is

69    known about which frequencies preferentially evoke rapid reaching responses. Here, we

70    systematically varied the spatial frequency of peripheral reach targets while measuring EMG

71    activity on an upper limb muscle. We found that visual stimuli composed of low-spatial

72    frequencies elicit the most rapid and robust EMG responses and corrective reaches. Thus, when

73    time is of the essence, low spatial frequencies preferentially drive fast visuomotor responses.

74

**Introduction**

75

76 To reach towards a visible target, visual information is ultimately transformed into motor

77 commands. Doing so requires extraction of visual attributes such as the color, shape, and size of

78 a visible target, and integration of these features into a command that is relayed to the motor

79 periphery typically via the corticospinal tract. However, there are instances where we have to

80 respond as quickly as possible, for example, to catch a falling mug or to volley a tennis ball that

81 deflects off the net during a tennis match. Which features of a visual stimulus best engender such

82 rapid visuomotor responses?

83 One way to study this question in the laboratory is to examine the latencies at which

84 participants respond to targets that are suddenly displaced during an on-going reaching

85 movement. In such dynamic scenarios, humans can initiate on-line reach corrections within a

86 remarkably short latency of ~125 ms following the target displacement (Soechting and

87 Lacquaniti, 1983; Day and Lyon, 2000). Veerman and colleagues (2008) systematically

88 investigated the influence of visual attributes in online reach corrections, and reported that earlier

89 responses were driven by stimuli defined by luminance, orientation, and size, but not other

90 attributes such as color. These results demonstrate that some visual attributes, but not others, are

91 crucial for these rapid online reach corrections.

92 Recently, we have described a novel way of investigating rapid visuomotor responses

93 which can be studied from a static posture. *Stimulus-locked responses* (SLRs) are short-latency

94 bursts of directionally-tuned electromyographic (EMG) activity that evolve time-locked within

95 ~100 ms of stimulus onset (Pruszynski et al., 2010), persisting even if an eventual reach is

96 withheld (Wood et al., 2015; Atsma et al., 2018). Although never studied in the same paradigm,

97 there are many similarities in the response properties of SLRs and on-line corrections. For

98 example, both SLRs (Gu et al., 2016) and the trajectory of the initial phase of on-line corrections

99 (Day and Lyon, 2000) are inexorably drawn toward the visual target, even when participants are

100 instructed to move in the opposite direction. We and others have hypothesized that SLRs, and by

101 extension the initial phase of an on-line reach corrections, are the product of a tecto-

102    reticulospinal pathway that is mediated through the intermediate and deep layers of the superior

103    colliculus (SCi) (Pruszynski et al., 2010; Corneil and Munoz, 2014). Consistent with this, SLRs

104    (Wood et al., 2015), online reach corrections (Veerman et al., 2008), and visual responses within

105    the SCi (Marino et al., 2012), are all evoked at a shorter latency by high contrast stimuli.

106          The current study was motivated by a recent paper which reported that visual responses

107    in the SCi responses are dependent on the spatial frequency (SF) of a visual stimulus, with SCi

108    neurons responding sooner to lower SFs (Chen et al., 2018). Our hypothesis that the visual

109    response in the SCi drives both the SLR and the earliest component of on-line reach corrections

110    predicts that both SLRs and on-line reach corrections should evolve sooner for lower SF stimuli.

111    We test this prediction in two experimental frameworks, measuring SLRs alone in reaches

112    starting form a static posture (*experiment 1*), and measuing both SLRs and on-line reach

113    corrections in a dynamic task where a reach target is displaced in mid-flight (*experiment 2*).

114    Consistent with our hypothesis, we find that rapid visuomotor responses, whether indexed by

115    SLRs or the latency of on-line reach corrections, are preferentially evoked by stimuli composed

116    of low SFs.

117

118    **Materials and methods**

119    *Participants*

120    A total of 33 participants (18 females, 15 males; mean age: 23.9 years SD: 3.4) completed at

121    least one of two experiments. All participants provided informed consent, were paid for their

122    participation, and were free to withdrawal from the experiment at any time. All but two

123    participants were right-handed. All participants had normal or corrected-to-normal vision, with

124    no current visual, neurological, or musculoskeletal disorders. All procedures were approved by

125    the Health Science Research Ethics Board at the University of Western Ontario.

126

127    *Apparatus*

128     Participants were seated in a KINARM robotic exoskeleton (BKIN Technologies, Kingston, ON,

129     Canada), and performed reaching movements with their right arm (**Fig. 1a**). As previously

130     described (Scott, 1999; Pruszynski et al., 2008), this robot permits arm movements in a

131     horizontal plane via shoulder and elbow flexion and extension, and allows for torque application

132     at these joints. Visual stimuli were projected from a downward facing LED monitor (LG

133     47LS35A, size: 47" resolution: 1920x1080 pixels), onto an upward facing mirror. A shield

134     underneath the mirror occluded direct vision of the hand, but real-time hand position was

135     represented on the monitor via a black dot with a diameter of 1 cm. A photodiode was used to

136     indicate the precise time of onset of the peripheral visual stimulus, and all kinematic and

137     electromyographic (EMG) data were aligned to photodiode onset. Eye movements were not

138     measured.

139

140     *Experimental design:*

141     *Experiment 1a: Static Task*

142     Participants (*n*= 16) performed visually guided reaches (**Fig. 1a,b**) towards peripheral stimuli

143     composed of stationary Gabor patches (see below), starting from a static posture in which the

144     hand was not in motion. Throughout the experiment, a constant torque of 2 Nm was applied to

145     the shoulder for the entire experiment, increasing tonic activity on the muscle of interest. Doing

146     so allowed for observations in decreases of muscle recruitment when the arm moved in the non-

147     preferred direction for the muscle of interest. Participants initiated each trial by bringing their

148     hand into a central black stimulus, which was located 45ccm in front of them relative to their

149     midline. This central stimulus had a 1 cm diameter and changed to white once the hand attained

150     this position. Participants were instructed to foveate this start position before target onset. The

151    trial was reset if the hand exited the start position before completion of a hold period

152    (randomized from 1-1.5 s). Simultaneous with the disappearance of the start position stimulus, a

153    Gabor patch subtending 7 cm then appeared either 10 cm to the left or right of the start position;

154    the center of this patch was at an eccentricity of ~9° to the left or right of the start position;

155    subtending approximately 12°. The Gabor patch was composed of one of six spatial frequencies

156    (SF) ranging between 0.15 to 2.22 cycles per degree (cpd) (**Fig. 1b**; see below for details on how

157    Gabor patches were constructed). Our lowest SF was implemented as a control target, as we

158    presented a very low SF, effectively presented as a gaussian blurred black dot. Participants were

159    instructed to reach towards the peripheral target as quickly as possible, with the trial ending

160    when the virtual cursor made contact with the Gabor. There were 12 unique trial conditions (six

161    SFs, each presented to the left and right). Participants completed five blocks of 240 trials each,

162    with each block containing 20 repetitions of each unique trial condition presented

163    pseudorandomly without replacement, yielding a total of 100 trials for each unique trial

164    condition.

165

166    *Experiment 1b: Static task with higher SF targets*

167    In experiment 1b, peripheral targets were placed at an increased distance from the subject,

168    permitting the presentation of higher spatial frequencies than in experiment 1a. Stimuli were

169    placed at locations resembling those used in experiment 2 (see below), so that the location of the

170    targets relative to the eye and hand were approximately the same in experiments 1b and 2. 16

171    participants, some of whom participated in experiment 1a, also participated in experiment 1b

172    (**Fig. 1a,b**). 14 of 16 participants in experiment 1b also participated in experiment 2 (see **Fig. 2b**

173    for participant details).

174    Participants initiated each trial by bringing their hand into a start position (2 cm diameter)

175    located 55.5 cm in front of them. A constant torque of 3Nm was applied to the shoulder for the

176    entire experiment. A higher torque was used than in experiment 1a, as target positions were less

177    in the preferred direction of the muscle. A fixation cross then appeared 10 cm above the central

178    hold marker, which participants were instructed to look at while not moving their hand.

179    Participants were required to maintain the initial hand position for a randomized period of 1-2

180    seconds. After this, a 5 cm diameter Gabor patch composed of one of three frequencies (.56,

181    2.22, 4.44 cpd; **Fig. 1b**) subtending approximately 4.5° of visual angle, was presented. The

182    center of this patch was ~8° of visual angle to the left or right of the start position. Participants

183    were instructed to reach and look to this peripheral target as quickly as possible. Participants

184    completed four blocks of 150 trials each, with each block composed of 25 trials of each unique

185    trial condition (three SFs to the right and left), yielding a total of 100 repeats of each unique trial

186    condition.

187

188    *Experiment 2: Dynamic Task*

189    In experiment 2, participants (n = 14, all of whom also completed experiment 1b in the same

190    session) occasionally generated online corrections to stimuli that suddenly jumped to the left or

191    right just after the start of a reaching movement. We term this a dynamic task, as the hand was in

192    motion when the target stimulus was displaced, necessitating an online correction. Peripheral

193    stimuli were presented at the same screen locations as in experiment 1b, and initial eye and hand

194    positions were also dissociated. A constant torque was not applied during experiment 2, as

195    participants in pilot experiments found this load to be too difficult to maintain for the duration of

196    experiment 2.

197     Participants initiated each trial by first bringing their hand into a central hold position (38

198     cm in front of them), while they looked at a central fixation cross located 17.5 cm above the

199     central hold stimulus (**Fig. 1a,b**). The central hold stimulus for the hand was placed closer to the

200     participant in experiment 2 than in experiment 1b, as a longer reaching movement permitted

201     more time for a mid-flight correction. Further, this configuration meant that the mid-flight hand

202     position at peripheral target presentation closely resembled that used in experiment 1b.

203     Participants then maintained this dissociated hand and eye position for 1-2s. After this, the

204     central fixation cross changed to a Gaussian blurred black dot, cueing the participant to reach

205     toward this central location. All trial types were identical up to this time. On 1/3$^{rd}$ of all trials

206     (termed control trials), no other event occurred and participants were simply required to reach

207     towards the gaussian blurred black dot. On the remaining 2/3rds of all trials (termed jump trials),

208     the blurred Gaussian black dot was replaced by a peripheral target identical to those used in

209     experiment 1b. The presentation of this peripheral target occurred when the hand exited the

210     central hold position (1 cm diameter), requiring participants to adjust an on-going reach

211     movement to either the left or right. Participants were instructed to reach as quickly as possible

212     to the fixation target on control trials, and to try to correct their reach movements as quickly as

213     possible on jump trials, so that they could move through the bottom aspect of the peripheral

214     Gabor patch. There was a total of seven unique trial combinations: a control trial, and six

215     different jump trials (three SFs per direction). Participants completed four blocks of 225 trials

216     each, with each block composed pseudorandomly of 75 control trials and 25 repeats of each

217     unique jump trial condition; thus, there were a total of 300 control trials and 100 trials of each

218     unique jump trial condition.

219

220    *Composition of peripheral Gabor target patches*

221    All stimuli were created in Matlab using the Psychophysics toolbox (Brainard, 1997; Pelli,

222    1997). Due to monitor resolution and the viewing distance of the targets, we were limited to an

223    upper limit of 2.22 cpd in experiment 1a, and 4.44 cpd in experiment 1b and 2. Stimuli consisted

224    of vertical sinewaves overlaid with a Gaussian window. In all experiments, peripheral target

225    stimuli consisted of perceptually contrast matched Gabor patches varying in SF measured in cpd

226    of visual angle. Our motivation to implement a contrast matching procedure was two-fold. First,

227    we performed this procedure in an attempt to isolate the effects of SF from perceived contrast, as

228    contrast influences SLR latency and magnitude (Wood et al., 2015). Second, perceptual contrast

229    matching mitigates some of the increases in RT with higher SFs (Breitmeyer, 1975), which was

230    important given that larger magnitude SLRs precede shorter RTs (Pruszynski et al., 2010; Gu et

231    al., 2016). We used a modified contrast matching procedure with foveal stimuli as described in

232    (Davidson, 1968). A double random interleaved procedure was used for each SF, on a linearized

233    (gamma-corrected) screen (mean background luminance 42.78 cd/m2). Participants were

234    presented a fixation point, followed by a flashed Gabor patch (200 ms), followed by a pause of

235    500 ms, followed by a second flashed Gabor patch (200 ms); participants were instructed to

236    "indicate the stimulus with more contrast", by button press. In each experiment, we used a single

237    standard stimulus presented at a suprathreshold 85% contrast from the middle SF used in each

238    experiment, with the comparison stimulus from each of the SFs being composed of a Gabor

239    patch presented at a higher or lower contrast, as determined by a staircase procedure. Our

240    rationale for using suprathreshold contrast is based on the relationship between SLR detectability

241    and contrast (Wood et al., 2015). After a reversal (participant changes response from increasing

242    to decreasing contrast or vice versa), the step size was decreased. Each staircase procedure

243  required ten reversals, and the contrast for a matched stimulus was taken as the mean contrast of

244  the last five reversals. All participants completed this procedure for all SFs used in a given

245  experiment, yielding a unique set of perceptually contrast-matched Gabors across a range of SFs

246  for each subject, which were then used in the experiment.

247

248  *Data acquisition and analysis*

249  As previously described (Gu et al., 2018), surface electromyographic (EMG) activity was

250  recorded from the clavicular head of the right pectoralis muscle with double-differential surface

251  electrodes (Delsys Inc. Bagnoli-8 system, Boston, MA USA). We placed two electrodes on each

252  participant, and chose the recording exhibiting the higher level of background activity. EMG

253  signals were sampled at 1,000 Hz, amplified by 1000, and rectified off-line. We excluded data

254  from three participants (one from experiment 1a, two from experiment 1b, and four from

255  experiment 2) due to an absence or very low level of recruitment for movements in the preferred

256  direction of the muscle. We used the same muscle recordings in all but three participants

257  between experiments 1b and 2.

258      All kinematic data were sampled at 1000 Hz by the Kinarm data acquisition system.

259  Reaction time (RT) was calculated as time from peripheral target appearance (measured by the

260  photodiode) to the initiation of the reaching movement. In all experiments, reach initiation was

261  determined using the lateral velocity towards left and right targets, extrapolating a line drawn

262  between the crossings of 25% and 75% of single trial peak velocities back to zero (as in

263  (Veerman et al., 2008)).

264      Our previous work on upper limb muscle recruitment during visually-guided reaching has

265  distinguished the small burst of EMG activity aligned to stimulus onset (i.e., the SLR) from the

266    larger, later burst of EMG activity associated with onset of the reaching movement (Gu et al.,

267    2016, 2018). The distinction between the SLR and the later movement-related burst becomes

268    blurred for shorter-RT movements. Given that the goal of this manuscript is to isolate the effects

269    of the spatial frequency of a peripheral stimulus on the SLR, we excluded trials below a

270    particular RT (excluding trials with RTs < 185 ms in experiments 1a and 1b, and trials with RTs

271    < 150 ms in experiment 2), since RTs of on-line reach corrections tend to be shorter than RTs

272    initiated from a static posture. In all experiments, we also excluded trials with RTs > 500 ms, due

273    to presumed inattentiveness. Finally, in all experiments, we excluded trials where the hand

274    deviated by more than 2 cm in the wrong direction (<1% of all trials).

275          We used a receiver-operating characteristic (ROC) analysis to quantitatively define the

276    presence and latency of the SLR, as described previously (Corneil et al., 2004; Pruszynski et al.,

277    2010). We separated EMG activity based on stimulus location and SF condition. EMG activity

278    for the same SF but opposite stimulus locations was then analyzed at every time sample (1 ms)

279    between 100 ms before and 300 ms after stimulus presentation. For each sample we calculated

280    the area under the ROC curve, which indicates the probability that an ideal observer could

281    discriminate between leftward and rightward stimulus presentations based solely on the EMG

282    activity. A value of .5 indicates chance discrimination, whereas values of 1 or 0 indicate

283    perfectly-correct or incorrect discrimination, respectively. Discrimination threshold was set to

284    0.6, which corresponds approximately to the upper 95% confidence interval determined using a

285    bootstrapping procedure (Goonetilleke et al., 2015). ROC latency was defined as the time where

286    the ROC time series surpassed threshold and remained above it for a minimum of eight out of ten

287    samples.

288    A representation of trial-by-trial EMG activity, mean EMG, and the associated time-

289    series ROC analysis which we use to define SLR characteristics is shown for a representative

290    participant in **Fig. 1c-e**. The SLR is visible in this example as a vertical banding indicating a

291    change in muscle recruitment aligned to stimulus as opposed to movement onset (**Fig. 1c**), and as

292    a transient increase or decrease in activity in mean EMG activity for leftward and rightward

293    stimuli, respectively (**Fig. 1d;** highlighted by the grey boxes). To determine if the initial change

294    in EMG activity was more locked to stimulus onset than movement onset, for each SF we

295    performed a median-split of trials based on RT and conducted separate ROC time-series analyses

296    for both 'early RT' (i.e., the subset of shorter RT trials) and 'late RT' (the subset of longer RT

297    trials) subsets (Goonetilleke et al., 2015; Wood et al., 2015). We then calculated the slope of the

298    line connecting the average RT and the SLR latency for the 'early' and 'late' RT sub-groups (see

299    **Fig. 3c** for examples).  Participants were classified as exhibiting a SLR if the slope of the line

300    exceeded 67.5 degrees, which is halfway between a line parallel to the line of unity (45 degrees)

301    and vertical (90 degrees); a slope > 67.5 degrees indicates that EMG recruitment was more

302    locked to stimulus rather than movement onset. If a SLR was detected using the median split

303    analysis, a subsequent time-series ROC plot was constructed using all trials to determine the

304    SLR latency (the first of 8 of 10 consecutive points > 0.6) and the SLR magnitude (defined as the

305    area between leftward and rightward mean EMG traces calculated from interval spanning from

306    the SLR latency to 15 ms later).

307    In experiment 2, we also conducted a time-series ROC analysis to determine the latency

308    of on-line reach corrections, based on the lateral position of the manipulandum (position along

309    the x axis) towards leftward or rightward stimuli on jump trials. As with the analysis of EMG

310    activity, the threshold was set to 0.6, and the latency was determined as the first of 8 of 10

311    consecutive points exceeding this threshold. We also defined the magnitude of the reach

312    correction as the area between the mean trajectories for left and right reach corrections in an

313    interval spanning from the time of discrimination to 400 ms after stimulus onset. Thus, larger

314    magnitudes are indicative of an increased ability to move laterally towards a target.

315

316    *Statistical analyses*

317    Statistical analyses were performed in MATLAB (version R2016a, The MathWorks, Inc.,

318    Natick, Massachusetts, United States). Results were analyzed with paired t-tests or one-way

319    repeated measures ANOVAs, unless otherwise stated, and post-hoc tests were Bonferroni

320    corrected where appropriate. Chi-squared tests were used to analyze changes in SLR prevalence

321    across SF.

322

323    **Results**

324    *Higher spatial frequencies elicit longer reaction times*

325    We first quantified the influence of the spatial frequency (SF) of a stimulus on reaction time

326    (RT), across all experiments and participants. Participants performed reaches from a static hand

327    position to stimuli placed either right or left of a start position (experiment 1a; **Fig 1a,b**), right-

328    outward or left-outward of a start position (experiment 1b; **Fig 1a,b**), or performed on-line reach

329    corrections of an outward reach movement to targets displaced to the left or right (experiment 2;

330    **Fig 1a,b**). As expected based on Breitmeyer (1975), and even with the perceptual contrast-

331    matching procedure, in all experiments we found that the SF of a stimulus influenced RTs (one-

332    way repeated measures ANOVA of mean RT; Experiment 1a; $F_{(5,75)} = 69.44$  $p=9.83^{-27}$; **Fig 2a**

333    top panel; Experiment 1b; $F_{(2,30)} = 134.04$  $p= 1.10^{-15}$; **Fig 2a** middle panel; Experiment 2; $F_{(2,26)}$

334    $= 99.68$  $p= 6.42^{-13}$; **Fig 2a** bottom panel). As shown in **Fig. 2a**, RTs tended to increase for

335    higher SFs (post-hoc analyses via paired t-tests Bonferroni-corrected for multiple comparisons;

336    the only insignificant comparison between adjacent SFs were between 0.15 vs 0.3 cpd and 0.3 vs

337    0.6 cpd in experiment 1a). Importantly, RT distributions for a given SF and the next-highest SF

338    often overlapped. In a subsequent analysis, we will exploit this overlap and mitigate the potential

339    confound of RT on the SLR.

340

341    *Earlier SLRs are preferentially evoked by lower SFs*

342    Next, we examined the influence of the SF of a stimulus on SLR characteristics. As shown in

343    previous work, the SLR on limb muscles consists of a brief increase or decrease in the

344    recruitment of muscle activity (~100 ms) (Pruszynski et al., 2010). **Fig. 1c** shows one example of

345    a prominent SLR in one representative subject from Experiment 2, who generated leftward or

346    rightward visually-guided corrections to a .56 cpd displaced target. In this example, the SLR

347    appears as the prominent vertical band of EMG activity that begins ~90 ms after visual target

348    presentation, regardless of the ensuing reaction time (see **Figs. 3** and **4** for other examples of

349    SLRs).

350         We used a time-series ROC analysis (see Methods) to detect the presence or absence of

351    an SLR. A participant was deemed to exhibit an SLR at a particular SF if the slope of a line

352    connecting the reaction time plotted as a function of the discrimination time for the early and late

353    RT groups exceeded 67.5 deg (indicating EMG activity is more locked to stimulus onset as

354    opposed to movement onset). Using this analysis, we detected an SLR+ observation in at least

355    one SF condition in 12 out of 16 participants in experiment 1a (**Fig. 2b** top panel; see **Fig. 3** for

356    data from a representative subject for experiment 1a), 11 out of 16 participants in experiment 1b

357    (**Fig. 2b** middle panel; see **Fig. 4a-c** for data from a representative subject for experiment 1b),

358  and 12 out of 14 participants in experiment 2 (**Fig. 2b** bottom panel; see **Fig. 4d-f** for data from a

359  representative subject for experiment 2). The data shown in **Figs. 3** and **4** also shows a

360  qualitative pattern whereby lower SFs evoke shorter latency and more distinct SLRs when

361  compared to SLRs evoked by higher SFs (e.g. 0.15 cpd versus 1.6 cpd rows in **Fig. 3**, .56 cpd

362  versus 2.22 cpd **Fig. 4)**.

363       To quantify the influence of the SF of a stimulus on the SLR across our sample, we

364  examined how the prevalence, latency, and magnitude of the SLR change as a function of SF.

365  Prevalence measures the proportion of participants exhibiting an SLR at a particular SF. As

366  shown in the top row of Fig, 5, SF influenced SLR prevalence in all experiments, with either the

367  lowest SF (experiments 1b and 2) or second lowest SF (experiment 1a) being associated with the

368  greatest prevalence, which was significantly different than the prevalence at the highest SF (chi-

369  squared test; experiment 1a: $p$=.012, chi-squared= 6.35, df= 1; experiment 1b: $p$=.013, chi-

370  squared= 6.15, df= 1; experiment 2: $p$=8.01^-5, chi-squared= 15.56, df= 1).

371       As shown in **Fig. 2e**, not all participants exhibited SLRs in each SF condition. This

372  creates an unbalanced design which complicates the analysis of how the characteristics of the

373  SLR vary as a function of SF. To analyze how SLR latency changed as a function of SF in

374  experiment 1a, we split SLR+ observations into 'low' (.15, .3, .6 cpd) and 'high' (1.11, 1.6, 2.22

375  cpd) groups. For each participant, we then took the mean of any latency from an SLR+

376  observation for each of the 'low' versus 'high' groups, and analyzed results from participants

377  exhibiting at least one SLR+ observation in both of the low and high conditions. For experiment

378  1b and 2, we analyzed results from any participant exhibiting an SLR+ observation at more than

379  one SF. All experiments revealed an influence of stimulus SF on the latency of the SLR, with

380  lower SFs eliciting shorter-latency SLRs (paired t-tests; Experiment 1a: t(9)= -5.37  $p$=.00045,

381 **Fig. 5a** bottom panel; Experiment 1b: t(5)= -3.64  $p$=.015; **Fig. 5b** bottom panel; Experiment 2:

382 t(3)= -6.13  $p$=.0087, **Fig. 5c** bottom panel).

383        We attempted to conduct a similar analysis on the magnitude of the SLR response, but

384 such an analysis was complicated by the increases in SLR latency that we observed for higher

385 SFs. As a consequence, the large volley of EMG activity associated with movement-related

386 activity often overlapped with the SLR interval (e.g., see **Fig. 4d**, for the .56 versus 2.22 cpd

387 condition), obscuring the quantification of EMG recruitment attributable to the SLR. SLRs

388 tended to be easily distinguished at the lower but not higher SFs, as shown both by the vertical

389 banding tied to stimulus onset in trial-by-trial EMG activity, and a distinct initial peak or plateau

390 in the time-series ROC plots (see also Wood et al. 2015). In contrast, time-series ROC plots for

391 higher SF stimuli, regardless of whether they were classified as SLR+ or SLR-, tended to lack a

392 clear initial peak or plateau after discrimination (e.g., 2nd and 3rd rows of **Fig. 4e**). The lack of a

393 clear initial peak in the time-series ROC for higher SF stimuli reinforces our concerns about

394 whether an analysis of EMG recruitment during the SLR interval would fairly capture only

395 activity attributable to the SLR, rather than also including movement-related activity on some

396 subset of trials.

397        Overall, despite our inability to comprehensively quantify SLR magnitude in what we felt

398 was a fair manner uncontaminated by movement-related activity, in all experiments we observed

399 clear trends for lower SF stimuli to elicit shorter-latency and more robust SLRs.

400

401 *Latency and prevalence effects persist in results controlled for reaction time*

402 As described in the methods, all peripheral stimuli were perceptually contrast-matched across

403 SFs in an attempt to minimize potential perceptual confounds. Consistent with previous results,

404     although contrast matched, higher SFs elicited longer RTs (Breitmeyer, 1975). Could the

405     dependencies with SF noted in the previous section simply result from the generation of shorter

406     RTs at lower SFs? To address this potential confound, we conducted an RT matching procedure

407     in which we selected a subset of trials at different SFs with overlapping RTs. In the matching

408     procedure, leftward and rightward reach RT data from 'low' SFs (the .6 cpd stimulus in

409     experiment 1a, the .56 cpd stimulus in experiments 1b and 2) were matched to leftward and

410     rightward reach 'high' SFs data (the 2.22 cpd stimulus in all experiments), respectively. In the

411     first step of the matching procedure, we matched pairs of trials with identical RTs, without

412     replacement. We then iteratively identified pairs of trials with RTs within +/-15 ms of each other,

413     again without replacement, prioritizing the shortest RTs. Once this matching procedure was

414     completed, we only analyzed datasets with more than 45 RT-matched trials.

415             This procedure yielded distributions with very similar RTs for leftward or rightward

416     reaches across different SFs. The distributions of RTs matched in this way were not significantly

417     different in 31/32 comparisons for experiment 1a, 30/32 comparisons in experiment 1b, and

418     26/28 comparisons in experiment 2 ($t$-test, testing at $p < 0.05$, conservatively not correcting for

419     multiple comparisons). Of those few distributions where RTs were found to be different, mean

420     RTs differed by less than 8 ms. We then repeated our analyses of the SLR on this subset of trials,

421     closely-matched for RTs.

422             **Figure 6** shows EMG data and time-series ROC plots for a representative participant

423     from each of the three experiments. From these examples, it is clear that the dependency of SLR

424     with SF persists even with closely-matched RTs. For example, a clear SLR evolves after the

425     presentation of a lower SF stimulus in experiments 1a, 1b, and 2, but not at the higher SF.

426     Further, any features of EMG recruitment that appeared to be related to the higher SF stimulus

427     evolved ~30 ms later than to the low SF stimulus, despite closely matched RTs (e.g., **Fig. 6g**). In

428     these examples, the influence of SF on the earliest direction-dependent EMG activity is

429     particularly apparent in the mean EMG and time-series ROC plots shown in the right column of

430     **Fig. 6**, in that the divergence of EMG activity following leftward versus rightward target

431     presentation occurs earlier when the target is composed of low than high SFs (green versus

432     purple traces).

433        **Figure 7** shows SLR prevalence and latency across our sample for RT-matched data.

434     From this figure it is clear that lower SFs continued to elicit more prevalent (**Fig. 7a,c,e**) and

435     shorter latency (**Fig. 7b,d,f**) SLRs, even when RTs are closely matched. These results reached

436     significance for SLR prevalence in experiment 2 ($p$ = .018, chi-squared= 5.6, df=1), and for SLR

437     latency in experiment 1b (t-test; $t_{(15)}$=-3.24, $p$ = .0054; **Fig. 7d**), and experiment 2 (t-test $t_{(8)}$=-

438     2.65, $p$ = .029; **Fig. 7f**). These analyses confirm that the dependencies of SLR responses

439     properties on the spatial frequency of a stimulus are not simply the result of short RTs to stimuli

440     composed of lower SFs.

441

442     *SLRs, and muscle recruitment more generally, evolve earlier when the arm is already in motion*

443     We noticed in **Figure 5** that SLR latencies were shorter when the arm was already in motion

444     (experiment 2) versus in a stable posture (experiment 1). Recall that experiments 1b and 2 were

445     configured so that the retinal location of peripheral targets, and the spatial position of the hand at

446     peripheral target onset, were approximately equal (**Fig. 1a,b**). Therefore, we investigated the

447     differences in SLR latency to the same stimulus between experiment 1b and 2. To do this, we

448     plotted the SLR latency in experiment 2 as a function of that in experiment 1b. As illustrated in

449     **Fig. 8a**, all but one participant response fell below the line of unity, indicating shorter SLR

450    latencies in experiment 2 (paired t-test, t(7)= 4.88  $p$=.0018). Thus, in those few instances where

451    an SLR was provoked to the same stimulus in both experiment 1b and 2 for the same participant,

452    shorter SLRs were observed when the hand was already in motion (22 ± 13 ms, n = 8). Note that

453    since these values are specifically locked to stimulus onset, this ~20 ms difference is not due to

454    the lower RT cutoff used in Experiment 2.

455        We also sought to determine the time at which EMG activity indicated the side of target

456    presentation, regardless of whether an SLR was detected or not. As shown in **Fig. 8b**, earlier

457    discrimination times persisted in experiment 2 across all participants and across all SFs (paired t-

458    test, t(41)=6.25, $p$ = 1.9e-7). Comparatively, we observed a smaller difference in discrimination

459    time in those observations that lacked an SLR in both the static and dynamic experiment (13 ±

460    15 ms shorter in experiment 2, n = 34). Interestingly, as seen in **Fig. 8b**, SF also appeared to

461    influence the comparative discrimination time, as the higher SFs clustered closer to the line of

462    unity (repeated measures ANOVA $F_{(2,26)}$ = 3.76  $p$= .037; **figure 8b**, red versus black

463    differences). Thus, when the arm is in motion, information related to target presentation gets to

464    the upper limb sooner. However, this effect is greatest in the presence of an SLR, and to low SF

465    stimuli.

466

467    *Paralleling SLRs, on-line reach corrections start earlier for lower SF stimuli*

468    All participants demonstrated a similar pattern of online corrections (**Fig. 9a**), wherein the lowest

469    SF evoked the shortest latency and largest magnitude corrections. Paralleling SLR responses, the

470    corrective latency systematically increased (one-way repeated measures ANOVA $F_{(2,26)}$ = 99.78

471    $p$=6.34e-13, **Fig. 9b**), and magnitude systematically decreased (one-way repeated measures

472    ANOVA $F_{(2,26)}$ = 437.86  $p$=9.52e-21, **Fig. 9c**) as a function of SF.

473     Experiment 2 offers the opportunity to examine SLRs, EMG recruitment more broadly,

474     and the parameters of on-line reach corrections in the same participants. Therefore, we collapsed

475     across conditions to examine a range of responses. We observed that the latency and the

476     magnitude of the online corrections were significantly correlated (Pearson's correlation, $R^2 = .79$,

477     $p = 2.27e{-}15$), indicating that earlier corrections related to larger lateral movement. Furthermore,

478     as would be expected in a muscle contributing to the on-line correction, the latency of EMG

479     discrimination was also significantly correlated with the latency of the reach correction

480     (Pearson's correlation, $R^2 = .77$, $p = 6.06e{-}15$), with EMG recruitment preceding kinematic

481     changes by 128 +/- 18 ms in experiment 2. As seen in **Fig. 10**, there was also a clear three-way

482     relationship between EMG responses, and the latency and magnitude of online reach corrections.

483     Thus, as expected, earlier changes in EMG recruitment were associated with earlier and larger

484     on-line reach corrections.

485     We also explored the relationship between the presence or absence of SLRs and online

486     reach behavior. Firstly, the impression from **Fig. 10** is that all the data across participants falls

487     along a smooth continuum, regardless of a response being SLR+ or not. Secondly, along this

488     continuum, SLR+ observations tended to cluster near the most rapid and largest online

489     corrections. To show this, we performed a *k*-means cluster analysis (with $k = 3$) and found that

490     SLRs predominated in the clusters associated with the earliest and largest corrections (SLR

491     prevalence of 73% (11/15), 35% (5/14), and 0% (0/13) as clusters increased in latency). Taken

492     together, earlier EMG responses led to earlier and larger online corrections. If evoked, SLRs

493     were associated with earlier and larger on-line corrections.

494

495

496     **Discussion**

497     To interact with our visual world, we are required to transform visual information into motor

498     commands. Here, we systematically investigated which spatial frequencies (SFs) preferentially

499     engender rapid visuomotor responses. We analyzed stimulus-locked responses (SLRs) on upper

500     limb muscles, as participants performed visually guided reaches towards either stationary targets

501     from a static posture, or targets abruptly displaced while a reaching movement is in mid-flight.

502     For all experiments, we found that low SFs elicited shorter latency and more prevalent SLRs.

503     Paralleling SLRs, online corrections started earlier for low SFs, and consequently attained

504     greater magnitudes. From this research, it is clear that a rapid visuomotor pathway preferentially

505     transforms low SF visual information into the earliest phases of muscle recruitment.

506

507     *A fast visuomotor system prefers lower spatial frequencies*

508     A variety of visual stimulus attributes, including stimulus color, intensity, and SF have also been

509     investigated in other rapid visuomotor responses such as saccadic RTs (Bell et al., 2006; White

510     et al., 2009; Chen et al., 2018) and ocular and manual following responses (Miles et al., 1986;

511     Carl and Miles, 1990; Saijo, 2005; Gomi et al., 2006). These results indicate that rapid

512     visuomotor responses rely heavily on the processing of some visual attributes, but not others.

513     Consistent with these findings, we demonstrate that the pathway mediating rapid EMG responses

514     and on-line corrections are preferentially sensitive to low SFs. Veerman and colleagues (2008)

515     studied the influence of many stimulus attributes on the latency of on-line corrections and found

516     that the shortest RT responses were generated in response to stimuli defined by contrast,

517     orientation, or size. Importantly, although Veerman and colleagues (2008) examined reactions to

518     a textured square, the dominant SF of the texture was not provided nor systematically varied. We

519    further this research and show that SLRs are preferentially evoked by low SFs which may be

520    elicited from either a static or dynamic limb position, and when present, are indicative of an

521    increased ability to correct ongoing reach behavior towards a target.

522

523    *Plausible neural substrates for SLRs and the initial phase of on-line reach corrections*

524    One potential structure that could serve as a sensorimotor interface for fast visuomotor responses

525    is the superior colliculus (SC), a midbrain structure involved in coordinating the orienting reflex

526    whereby an organism is able to rapidly realign the eyes, head, and upper body towards novel

527    stimuli of interest (see for review (Corneil and Munoz, 2014)). There are many similarities

528    between visual responses in the intermediate layers of the SC (SCi) and the SLR. For example, in

529    anti-saccade or anti-reaching tasks, visual responses in the SCi (Everling et al., 1999), and the

530    SLR on neck (Corneil et al., 2008) or limb muscles (Gu et al., 2016) are tuned to stimulus

531    location. Visual responses present in reach-related SCi neurons also correlate well with upper

532    limb muscle activity (Werner et al., 1997a, 1997b; Stuphorn et al., 1999), with SCi responses

533    preceding SLRs in neck muscles by approximately ~11 ms, consistent with the efferent lag from

534    the SCi to the neck (Rezvani and Corneil, 2008). Further, visual responses in the SCi (Li and

535    Basso, 2008; Marino et al., 2012), SLRs on the upper limb (Wood et al., 2015), and on-line

536    corrections (Veerman et al., 2008) all evolve at shorter latencies in response to high-contrast

537    visual stimuli, or low spatial frequencies ((Chen et al., 2018); current results). Indeed, SLRs have

538    been argued to resemble many aspects of express saccades (Corneil et al., 2004), when visual

539    responses in the SCi become strong enough to drive recruitment in the motor periphery.

540    Consistent with this perspective, express saccades have also been argued to occur at long

541     latencies to sub-optimal stimuli (Bell et al., 2006), which has been observed in SLRs towards

542     low contrast (Wood et al., 2015), or higher SF (**Fig. 5**) stimuli.

543           Our position is that SLRs, and by extension, the initial phase of online reach corrections

544     are mediated by visual responses in the SCi. While this idea is consistent with previous ideas of

545     how the SC may be involved in rapid visuomotor responses (Day and Brown, 2001), in general it

546     is thought that on-line reach corrections are driven through either parietal or frontal sources (for

547     review see (Gaveau et al., 2014; Archambault et al., 2015)). Although many of the stimulus

548     preferences for SLRs and on-line reach corrections resemble those reported in the SCi, we are

549     mindful that other areas in the parietal and frontal cortices implicated in on-line reach control

550     also exhibit visually-aligned response transients (Riehle, 1991; Cisek and Kalaska, 2005),

551     although the relationship between such transients and various stimulus features remain to be

552     investigated. The general similarities that we are observing between SLRs and the early phase of

553     on-line reach corrections suggests that a subcortical route involving the SCi may provide the

554     earliest drive to the motor periphery. Subsequent, more contextually-guided portions of the

555     online correction may rely on corticospinal inputs that incorporate processing in frontal and

556     parietal cortices.

557     *Expedited visuomotor responses when the limb is already in motion*

558     Experiments 1b and 2 were designed to compare SLRs in situations where stimulus presentation

559     occurred when the limb was either stable or already in motion. We found that SLRs, and the

560     earliest divergence of EMG activity, following stimulus onset evolved substantially earlier (~20-

561     30 ms) when the limb was already in motion. This observation relates to contemporary debates

562     about expedited RTs during movements initiated from a dynamic position (Smeets et al., 2015),

563     and are consistent with expedited responses occurring when a postural control policy has been

564    disengaged (Scott and Cluff, 2016). What is interesting is to consider *where* in the pathway

565    rapidly transforming vision into actions the delay in activity aligned to stimulus onset is delayed

566    by 20-30 ms when movements are beginning from a stable posture, and why such a delay

567    depends on SF. It would appear that any such delay would have to be imposed downstream from

568    the SCi, given that visual response latencies in the SCi approach the minimal afferent delay.

569

570    *Methodological considerations*

571    Our experimental configuration limited the upper range of SFs we could present without aliasing

572    (2.22 and 4.44 cpd in experiments1 and 2, respectively). We do not view this as a limitation, as

573    SLRs were rarely generated in response to a 4.44 cpd stimulus. Further, any SLRs that were

574    generated to the 4.44 cpd stimulus did so at a latency that overlapped with movement-related

575    activity. In this vein, the potential overlap between the SLR and movement-related activity

576    complicated analysis of SLR magnitude. Future experiments should investigate magnitude in a

577    paradigm which separates SLR and movement related activity, where immediate reaching is not

578    required. Interestingly, at the lower range of SFs in experiment 1a, we observed that the 0.15 cpd

579    stimulus elicited the shortest-latency but not necessarily the most prevalent SLR, highlighting

580    how these measures can be dissociated.

581        We went to some lengths to ensure the trends we observed in SLR latency and prevalence

582    across SFs were not confounded by RT, implementing a contrast-matching procedure and

583    reanalyzing SLRs after matching RTs. Our contrast-matching procedure also ensured that our

584    observed effects were due to the SF of the targets, as opposed to perceived contrast. However,

585    the on-line correction RTs we observed were longer than those reported previously (e.g., 125 ms

586    in (Day and Lyon, 2000). We surmise that there are a few reasons for this discrepancy. Firstly,

587     we observed single-trial examples with RTs below 200 ms (**Fig. 2a**), although we reported the

588     mean correction latencies. Secondly, we excluded shorter-latency RTs to prevent overlap with

589     movement-related activity. Most importantly, stimuli defined by texture are known to elicit

590     longer-RT corrections (Veerman et al., 2008).

591         Finally, SLR prevalence never exceeded 75%, meaning that stimuli did not always elicit

592     an SLR (see also Pruszynski et al., 2010; Wood et al., 2015; Gu et al., 2016). The failure to

593     observe an SLR may be due to participant idiosyncrasies, or to the possibility that the SLR

594     distributes to deeper layers of fatigue-resistant muscle (Pruszynski et al., 2010). As mentioned

595     above, Gabor patches may also be a suboptimal stimulus for the SLR. Recall also that our

596     classification criteria relied on a median-split analysis. This is a conservative approach that

597     requires a substantial number of trials and considerable variance in RTs.

598

599     *Conclusions*

600     The work presented here builds on a stream of findings that emphasize the importance of

601     stimulus attributes on visually-evoked responses in premotor areas and the motor periphery,

602     showing that the earliest component of a rapid visuomotor response is preferentially elicited by

603     low SF stimuli. The data from experiment 2 are the first to directly link the phenomenon of SLRs

604     to on-line reach corrections in the same task and in the same participants. This link will help

605     further characterizations of the substrates underlying rapid visuomotor responses, as the SLRs

606     can be readily elicited on a trial-by-trial basis while participants are in a stable posture. Detailing

607     the stimulus attributes which best elicit rapid visuomotor responses will help identify plausible

608     underlying substrates and will aid the study of such responses across the lifespan and in clinical

609     populations.

610    **Figure Legends**

611    **Figure 1.** Experimental design and SLRs. (**a, b**) General display and configuration of targets (**a**)

612    and corresponding hand and eye start positions, potential targets, go cues and spatial frequencies

613    used for each of the experiments (**b**; see Methods for more details). (**c**) Trial-by-trial recruitment

614    of right PEC for an example subject generated left or right reaches. Each row is a different trial,

615    with colour conveying degree of recruitment. Trials sorted by RT (white boxes), and aligned to

616    stimulus onset. The SLR (highlighted in grey vertical box) appears as a vertical banding of

617    increased or decreased recruitment aligned to left or right stimulus presentation, respectively,

618    rather than movement onset. (**d, e**) Mean EMG activity (+/- standard error; **d**) and time-series

619    ROC analysis (**e**) for data shown in (**c**). Horizontal dashed lines in e shows the 0.6 or 0.4 level

620    which constitutes discrimination threshold.

621

622    **Figure 2.** RTs and detection of SLRs. (**a**) Cumulative RT distributions in all experiments, pooled

623    across all participants and directions and segregated by SF. (**b**) Slope of the relationship between

624    discrimination time and average RT for early and late RT groups, for all experiments. Each data

625    point represents a unique subject for a particular SF. Slopes are capped at 90 deg. Results are

626    grouped into those who exhibiting an SLR in at least one condition (SLR+) or not (SLR-), given

627    a slope threshold of 67.5 deg (horizontal dashed line).

628

629    **Figure 3.** Example results from Experiment 1a. (**a**) Muscle recruitment from an example subject

630    from Experiment 1a, segregated by movement direction and SF. Same format as Fig. 1c. Trials

631    were separated into early (red) or late (blue) RT groups based on the median RT. (**b**) Time series

632    ROC plot analysis from early (red) or late (blue) RT groups for data in (**a**). Vertical coloured

633 solid lines depict discrimination time. (**c**) Plot of the average RT versus discrimination time for

634 early and late groups. The data was deemed to exhibit an SLR if the slope of the line exceeded

635 67.5 deg, which indicated that the initiation of EMG recruitment was more locked to stimulus

636 rather than movement onset.

637

638 **Figure 4.** Example results from the same participant in Experiment 1b (**a-c**) and 2 (**d-f**). Same

639 format as Fig. 3.

640

641 **Figure 5.** Effect of SF on latency and prevalence of the SLR, across all experiments and

642 participants. In each column, the top row conveys SLR prevalence (the percentage of SLR+

643 participants across the sample) as a function of SF, and the bottom row conveys SLR latency as a

644 function of SF. Error bars in lower row show standard error of mean. Asterisks depict differences

645 significant at the $p < 0.05$ level (see Results text for details).

646

647 **Figure 6.** Example results from all experiments for trials matched by RTs. Trial-by-trial EMG

648 activity (**a, d, g**; same format as Fig. 1c), mean EMG activity (**b, e, h**; same format as Fig. 1d),

649 and time-series ROC analysis (**c, f, i**; same format as Fig. 1e) for data from Experiment 1a (**a-c**),

650 Experiment 1b (**d-f**), and Experiment 2 (**g-i**). For each experiment, the RTs were matched for

651 individual trials following presentation of a stimulus of a low SF (purple) or high SF (green).

652 The solid boxes around the trial-by-trial plots depict data that exhibits an SLR, even with the

653 reduced number of trials.

654

655    **Figure 7.** The influence of SF on SLR characteristics persisted for RT-matched trials. Same

656    format as Fig. 5, using data matched for RT.

657

658    **Figure 8.** Discrimination times during on-line reach corrections (Experiment 2) plotted as a

659    function of discrimination times for reaches initiated from a static posture (Experiment 1b).

660    Discrimination times are derived from the time-series ROC analysis. Each data point depicts data

661    from a unique combination of subject and stimulus SF (see colour scheme). (**a**) Data from

662    occurrences with an SLR+ observation in both Experiments 1b and Experiment 2. (**b**) Data from

663    all participants, with symbols depicting whether SLRs were observed in both experiments (dots,

664    same data as in (a), but on a different time scale), whether an SLR was observed in only one

665    experiment (crosses), or whether an SLR was not observed in either experiment (asterisks). Solid

666    diagonal line shows line of unity. The clustering of data below the line of unity means that

667    shorter discrimination times were observed in Experiment 2.

668

669    **Figure 9. Characteristics of on-line reach corrections to different SFs in Experiment 2.** (**a**)

670    Results from a sample participant, depicting the mean lateral distance for on-line reach

671    corrections to displaced stimuli composed of different SFs (colored lines), or to the control

672    condition where the reach target was not displaced (black line). (**b, c**) Latency (b) or magnitude

673    (c) of on-line reach corrections across the sample, as a function of SF. The latency was derived

674    from a time-series ROC analysis of lateral distance for left versus right displaced stimuli. The

675    magnitude is normalized within each participant to the maximum correction. Error bars represent

676    SEM.

677

678   **Figure 10.** Three-way relationship between EMG discrimination, and the latency and magnitude

679   of the on-line reach correction. Each point represents data from a single participant, colour-coded

680   by SF, with the symbol indicating whether an SLR was observed (asterisks) or not (circles).

681

682

683

684

685

686

687

688

689

690

691

692

693

694

695 **References**

696    Archambault PS, Ferrari-Toniolo S, Caminiti R, Battaglia-Mayer A (2015) Visually-guided

697         correction of hand reaching movements: The neurophysiological bases in the cerebral

698         cortex. Vision Res.

699    Atsma J, Maij F, Gu C, Medendorp WP, Corneil BD (2018) Active Braking of Whole-Arm

700         Reaching Movements Provides Single-Trial Neuromuscular Measures of Movement

701         Cancellation. J Neurosci.

702    Bell AH, Meredith MA, Van Opstal AJ, Munoz DP (2006) Stimulus intensity modifies saccadic

703         reaction time and visual response latency in the superior colliculus. Exp Brain Res.

704    Brainard DH (1997) The Psychophysics Toolbox. Spat Vis 10:433–436.

705    Breitmeyer BG (1975) Simple reaction time as a measure of the temporal response properties of

706         transient and sustained channels. Vision Res 15:1411–1412.

707    Carl JR, Miles FA (1990) Short latency ocular-following responses in man. Vis Neurosci.

708    Chen CY, Sonnenberg L, Weller S, Witschel T, Hafed ZM (2018) Spatial frequency sensitivity

709         in macaque midbrain. Nat Commun.

710    Cisek P, Kalaska JF (2005) Neural correlates of reaching decisions in dorsal premotor cortex:

711         Specification of multiple direction choices and final selection of action. Neuron.

712    Corneil BD, Munoz DP (2014) Overt responses during covert orienting. Neuron 82:1230–1243.

713    Corneil BD, Munoz DP, Chapman BB, Admans T, Cushing SL (2008) Neuromuscular

714         consequences of reflexive covert orienting. Nat Neurosci 11:13–15

715    Corneil BD, Olivier E, Munoz DP (2004) Visual responses on neck muscles reveal selective

716         gating that prevents express saccades. Neuron 42:831–841.

717    Davidson M (1968) Perturbation Approach to Spatial Brightness Interaction in Human Vision*. J

718      Opt Soc Am.

719    Day BL, Brown P (2001) Evidence for subcortical involvement in the visual control of human

720       reaching. Brain.

721    Day BL, Lyon IN (2000) Voluntary modification of automatic arm movements evoked by

722       motion of a visual target. Exp Brain Res 130:159–168.

723    Everling S, Dorris MC, Klein RM, Munoz DP (1999) Role of primate superior colliculus in

724       preparation and execution of anti-saccades and pro-saccades. J Neurosci.

725    Gaveau V, Pisella L, Priot AE, Fukui T, Rossetti Y, Pélisson D, Prablanc C (2014) Automatic

726       online control of motor adjustments in reaching and grasping. Neuropsychologia.

727    Gomi H, Abekawa N, Nishida S (2006) Spatiotemporal tuning of rapid interactions between

728       visual-motion analysis and reaching movement. J Neurosci 26:5301–5308

729    Goonetilleke SC, Katz L, Wood DK, Gu C, Huk AC, Corneil BD (2015) Cross-species

730       comparison of anticipatory and stimulus-driven neck muscle activity well before saccadic

731       gaze shifts in humans and nonhuman primates. J Neurophysiol 114:902–913

732    Gu C, Pruszynski JA, Gribble PL, Corneil BD (2018) Done in 100 ms: Path-dependent

733       visuomotor transformation in the human upper limb. J Neurophysiol:jn.00839.2017

734    Gu C, Wood DK, Gribble PL, Corneil BD (2016) A Trial-by-Trial Window into Sensorimotor

735       Transformations in the Human Motor Periphery. J Neurosci 36:8273–8282

736    Li X, Basso MA (2008) Preparing to Move Increases the Sensitivity of Superior Colliculus

737       Neurons. J Neurosci 28:4561–4577

738    Marino RA, Levy R, Boehnke S, White BJ, Itti L, Munoz DP (2012) Linking visual response

739       properties in the superior colliculus to saccade behavior. Eur J Neurosci 35:1738–1752.

740    Miles FA, Kawano K, Optican LM (1986) Short-latency ocular following responses of monkey.

741     I. Dependence on temporospatial properties of visual input. J Neurophysiol.

742  Pelli DG (1997) The VideoToolbox software for visual psychophysics: transforming numbers

743     into movies. Spat Vis 10:437–442.

744  Pruszynski AJ, King GL, Boisse L, Scott SH, Randall Flanagan J, Munoz DP (2010) Stimulus-

745     locked responses on human arm muscles reveal a rapid neural pathway linking visual input

746     to arm motor output. Eur J Neurosci 32:1049–1057.

747  Pruszynski AJ, Kurtzer I, Scott SH (2008) Rapid Motor Responses Are Appropriately Tuned to

748     the Metrics of a Visuospatial Task. J Neurophysiol 100:224–238

749  Rezvani S, Corneil BD (2008) Recruitment of a head-turning synergy by low-frequency activity

750     in the primate superior colliculus. J Neurophysiol 100:397–411

751  Riehle A (1991) Visually induced signal-locked neuronal activity changes in precentral motor

752     areas of the monkey: hierarchical progression of signal processing. Brain Res.

753  Saijo N (2005) Large-Field Visual Motion Directly Induces an Involuntary Rapid Manual

754     Following Response. J Neurosci.

755  Scott SH (1999) Apparatus for measuring and perturbing shoulder and elbow joint positions and

756     torques during reaching. J Neurosci Methods 89:119–127.

757  Scott SH, Cluff T (2016) Online Corrections are Faster Because Movement Initiation Must

758     Disengage Postural Control. Motor Control 20:162–170.

759  Smeets JBJ, Wijdenes LO, Brenner E (2015) Movement Adjustments Have Short Latencies

760     because There Is No Need to Detect Anything. Motor Control.

761  Soechting JF, Lacquaniti F (1983) Modification of trajectory of a pointing movement in response

762     to a change in target location. J Neurophysiol.

763  Stuphorn V, Hoffmann KP, Miller LE (1999) Correlation of primate superior colliculus and

764    reticular formation discharge with proximal limb muscle activity. J Neurophysiol 81:1978–

765        1982

766    Veerman MM, Brenner E, Smeets JBJ (2008) The latency for correcting a movement depends on

767        the visual attribute that defines the target. Exp Brain Res 187:219–228.

768    Werner W, Dannenberg S, Hoffmann KP (1997a) Arm-movement-related neurons in the primate

769        superior colliculus and underlying reticular formation: Comparison of neuronal activity with

770        EMGs of muscles of the shoulder, arm and trunk during reaching. Exp Brain Res.

771    Werner W, Hoffmann KP, Dannenberg S (1997b) Anatomical distribution of arm-movement-

772        related neurons in the primate superior colliculus and underlying reticular formation in

773        comparison with visual and saccadic cells. Exp Brain Res.

774    White BJ, Boehnke SE, Marino R a, Itti L, Munoz DP (2009) Color-related signals in the primate

775        superior colliculus. J Neurosci 29:12159–12166

776    Wood DK, Gu C, Corneil BD, Gribble PL, Goodale MA (2015) Transient visual responses reset

777        the phase of low-frequency oscillations in the skeletomotor periphery. Eur J Neurosci
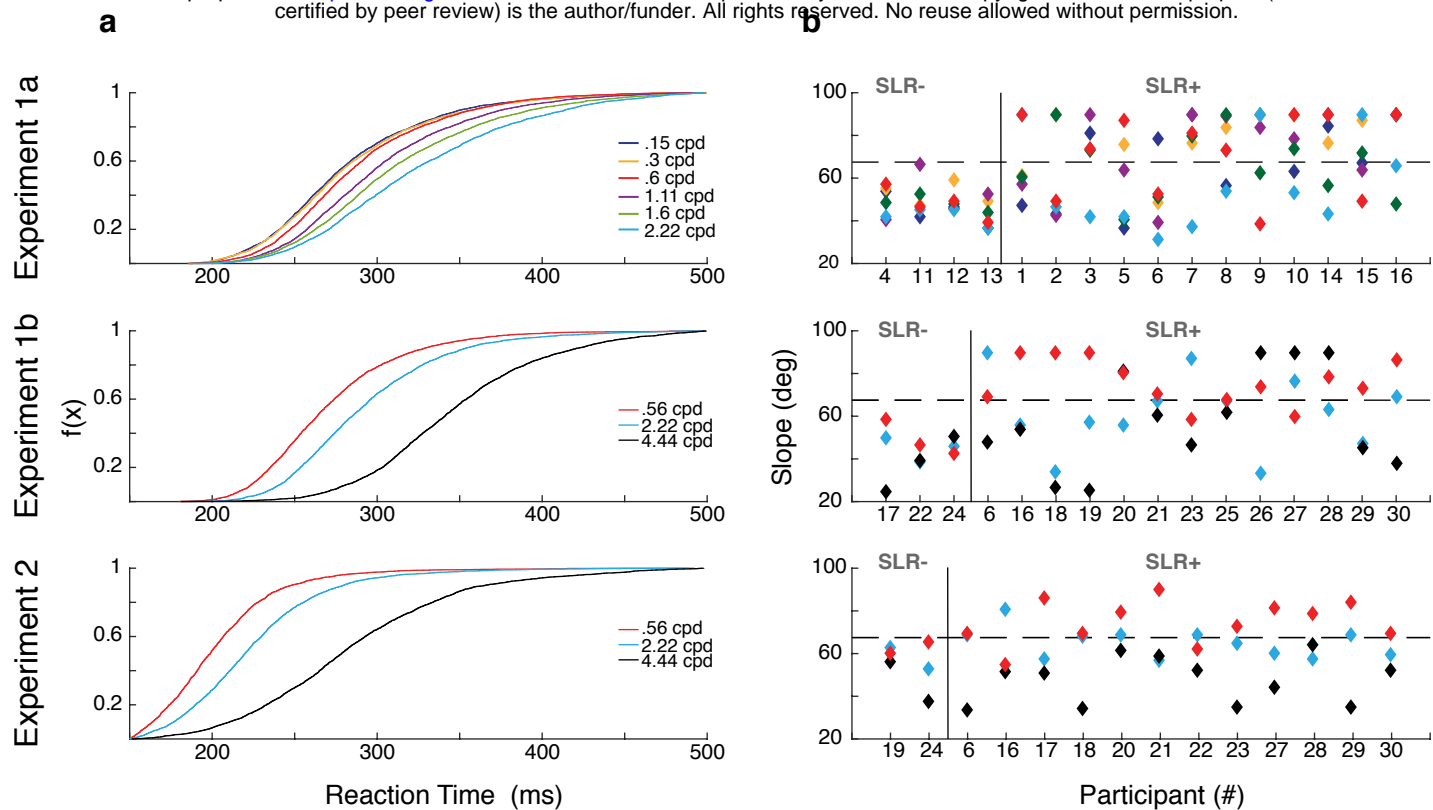
778        42:1919–1932.

779

**a**

**b**

| EXPERIMENT | START HAND | START EYE | POTENTIAL TARGETS | GO CUE | SPATIAL FREQUENCIES |
|---|---|---|---|---|---|
| 1A | A | A | 50% B, 50% C | Target Onset | .15, .3, .6, 1.11, 1.60, 2.22 cpd |
| 1B | D | E | 50% F, 50% G | Target Onset | .56, 2.22, 4.44 cpd |
| 2 | A | E | 33% E; 33% F; 33% G | E Onset | .56, 2.22, 4.44 cpd |

**c**

**d**

**e**
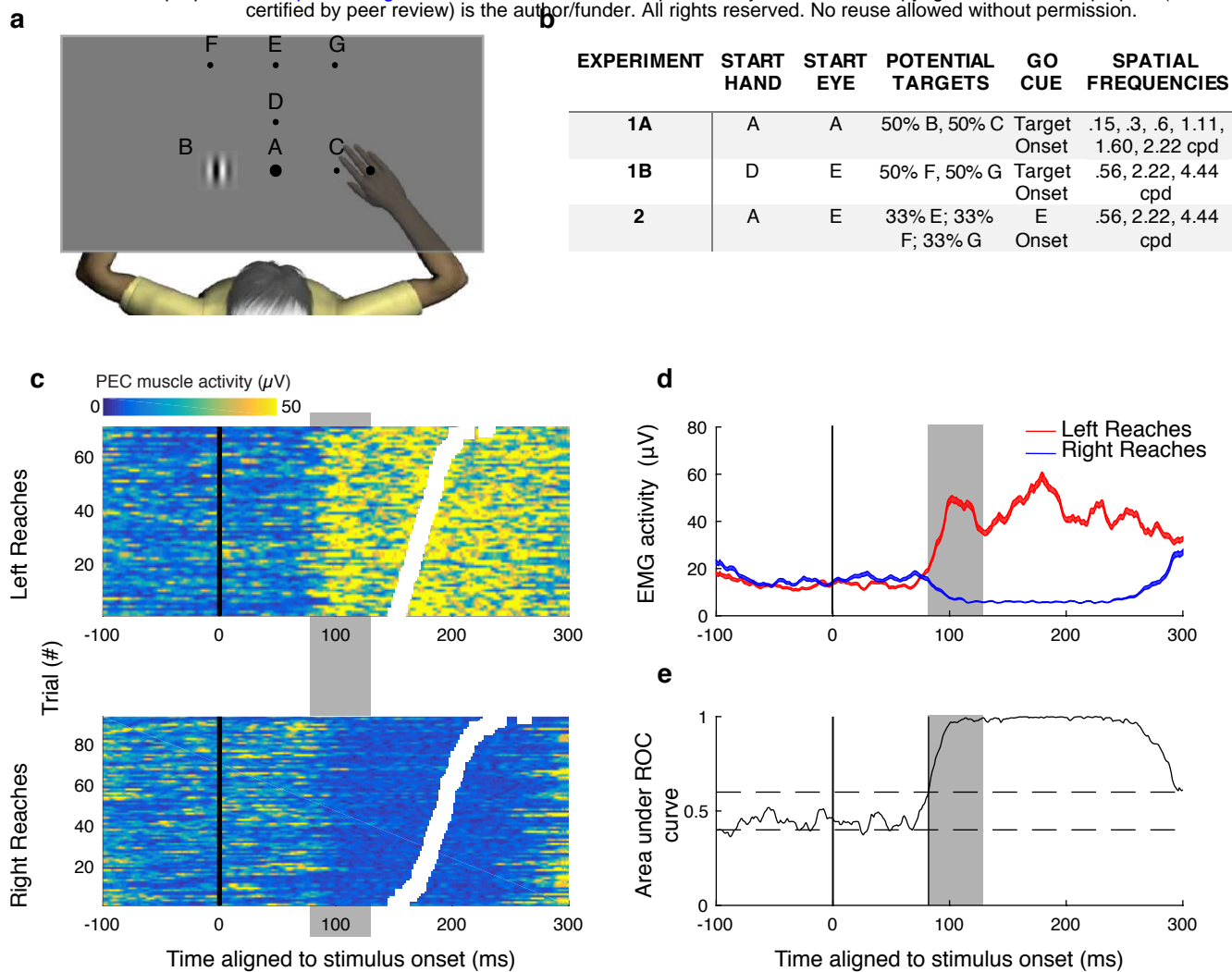


**Figure 1.** Experimental design and SLR classification. (a, b) General display and configuration of targets (a) and corresponding hand and eye start positions, potential targets, go cues and spatial frequencies used for each of the experiments (b; see Methods for more details). (c) Trial-by-trial recruitment of right PEC for an example subject generated left or right reaches. Each row is a different trial, with colour conveying degree of recruitment. Trials sorted by RT (white boxes), and aligned to stimulus onset. The SLR (highlighted in grey vertical box) appears as a vertical banding of increased or decreased recruitment aligned to left or right stimulus presentation, respectively, rather than movement onset. (d, e) Mean EMG activity (+/- standard error; d) and time-series ROC analysis (e) for data shown in (c). Horizontal dashed lines in e shows the 0.6 or 0.4 level which constitutes discrimination threshold.
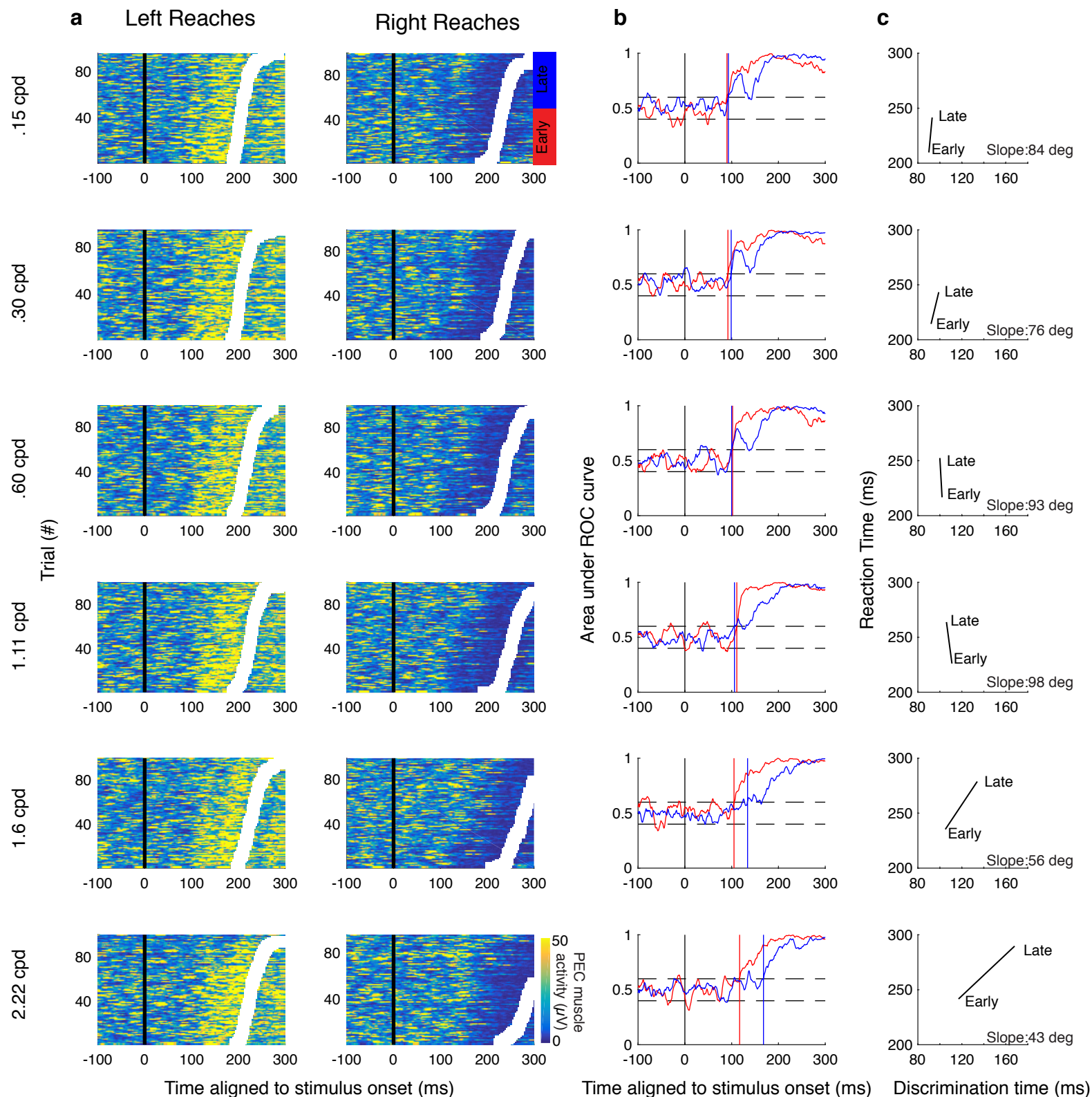
**Figure 2.** RTs and detection of SLRs. (a) Cumulative RT distributions in all experiments, pooled across all participants and directions and segregated by SF. (b) Slope of the relationship between discrimination time and average RT for early and late RT groups, for all experiments. Each data point represents a unique subject for a particular SF. Slopes are capped at 90 deg. Results are grouped into those who exhibiting an SLR in at least one condition (SLR+) or not (SLR-), given a slope threshold of 67.5 deg (horizontal dashed line).

**Figure 3.** Example results from Experiment 1a. (a) Muscle recruitment from an example subject from Experiment 1a, segregated by movement direction and SF. Same format as Fig. 1c. Trials were separated into early (red) or late (blue) RT groups based on the median RT. (b) Time series ROC plot analysis from early (red) or late (blue) RT groups for data in (a). Vertical coloured solid lines depict discrimination time. (c) Plot of the average RT versus discrimination time for early and late groups. The data was deemed to exhibit an SLR if the slope of the line exceeded 67.5 deg, which indicated that the initiation of EMG recruitment was more locked to stimulus rather than movement onset.
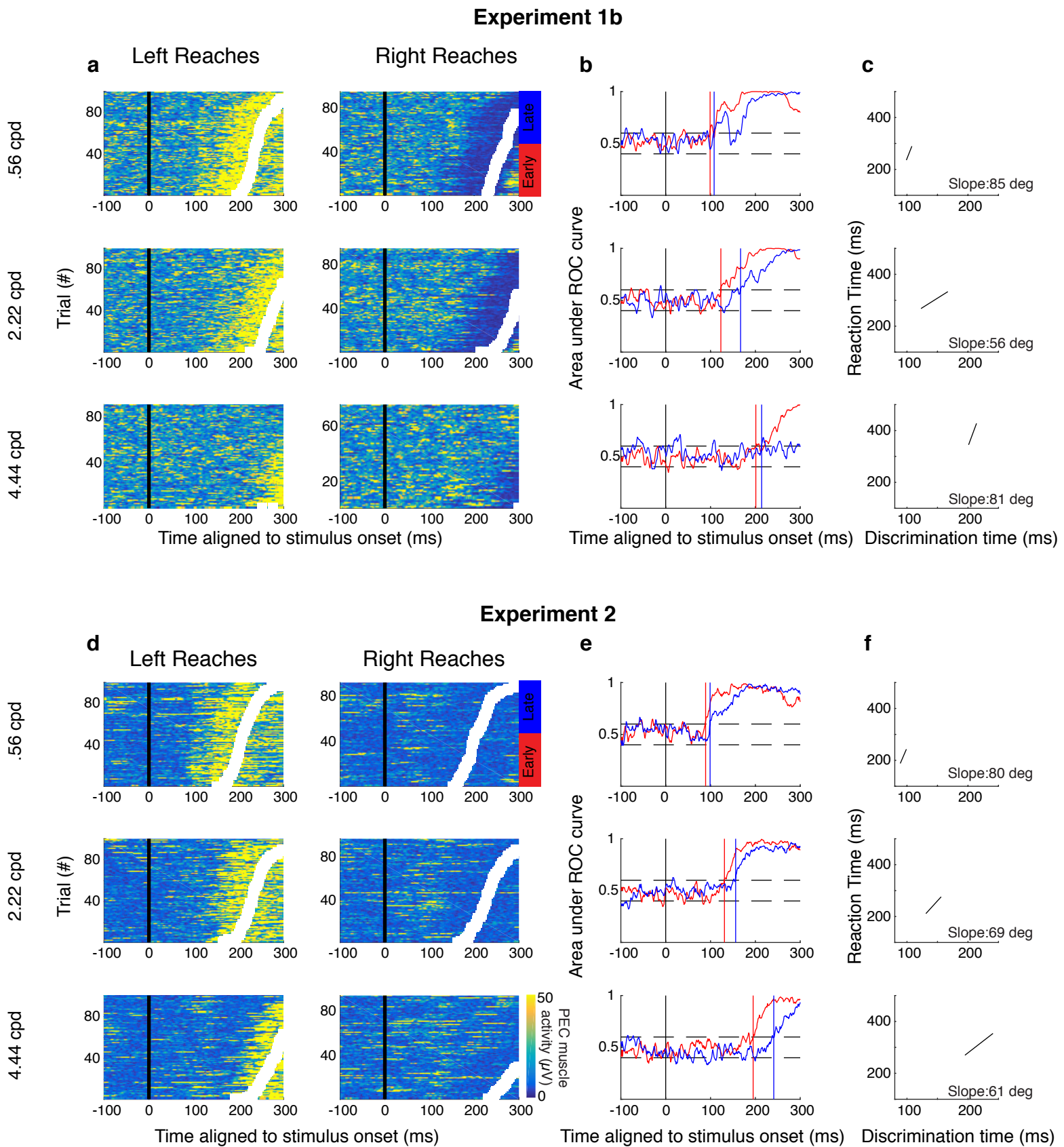
**Figure 4.** Example results from same subject in Experiment 1b (a-c) and 2 (d-f). Same format as Fig. 3.
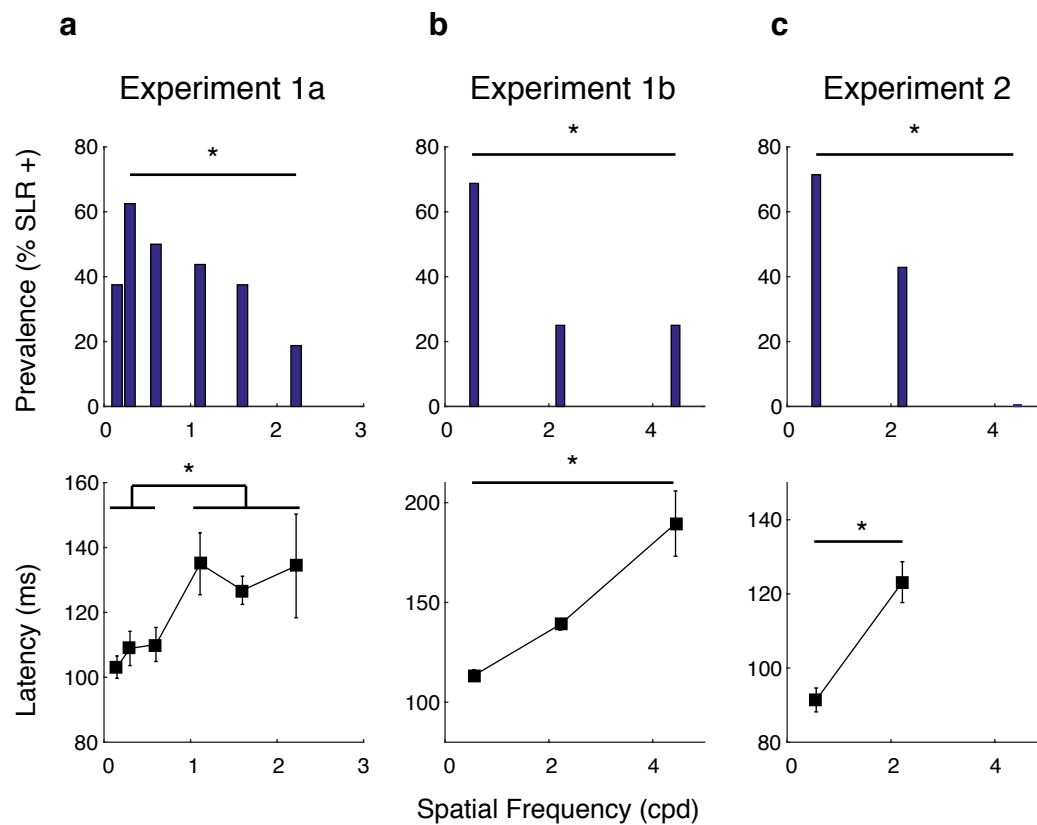
**Figure 5.** Effect of SF on latency and prevalence of the SLR, across all experiments and participants. In each column, the top row conveys SLR prevalence (the percentage of SLR+ participants across the sample) as a function of SF, and the bottom row conveys SLR latency as a function of SF. Error bars in lower row show standard error of mean. Asterisks depict differences significant at the $p < 0.05$ level (see Results text for details).
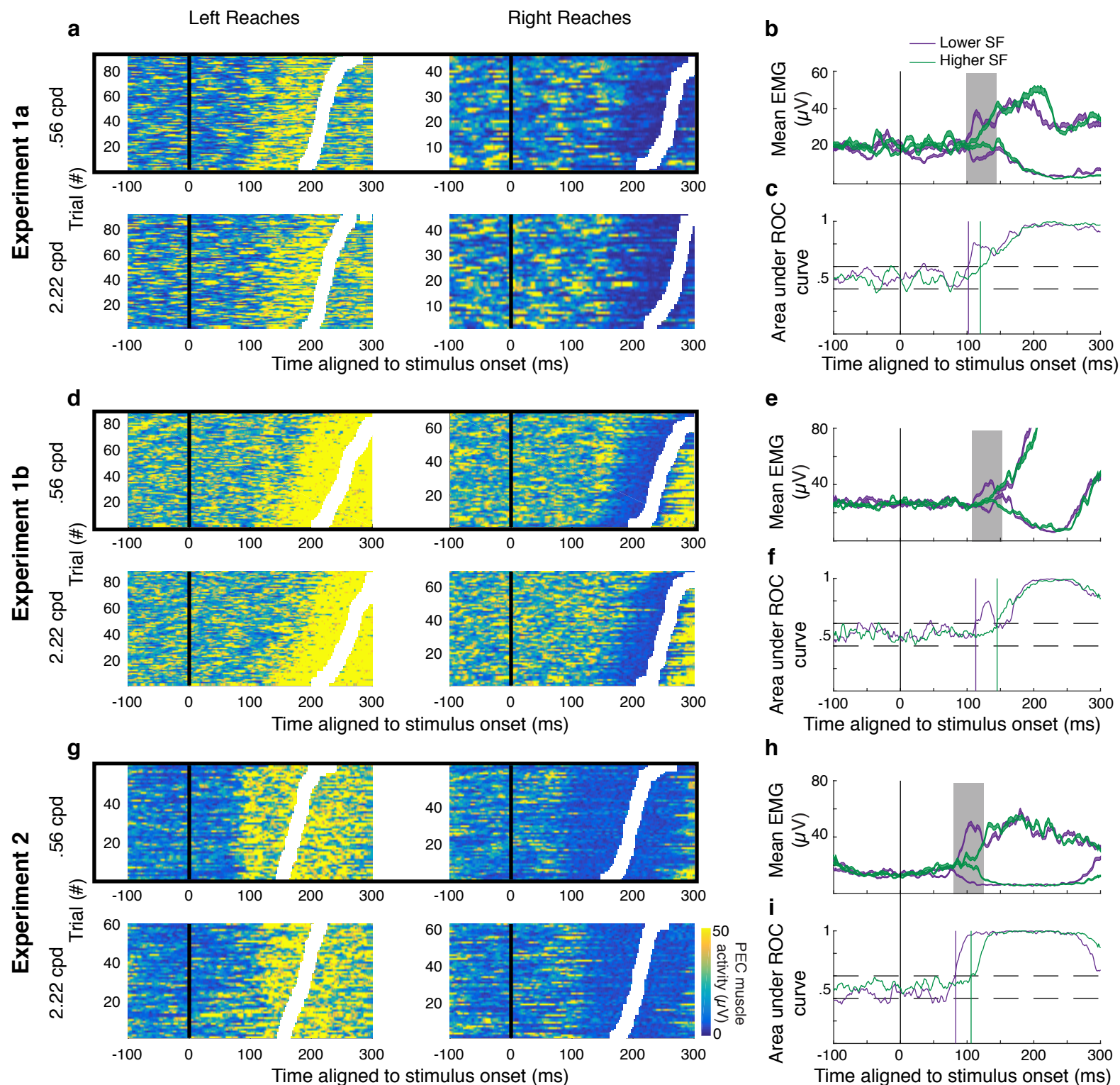
**Figure 6.** Example results from all experiments for trials matched by RTs. Trial-by-trial EMG activity (a, d, g; same format as Fig. 1c), mean EMG activity (b, e, h; same format as Fig. 1d), and time-series ROC analysis (c, f, i; same format as Fig. 1e) for data from Experiment 1a (a-c), Experiment 1b (d-f), and Experiment 2 (g-i). For each experiment, the RTs were matched for individual trials following presentation of a stimulus of a low SF (purple) or high SF (green). The solid boxes around the trial-by-trial plots depict data that exhibits an SLR, even with the reduced number of trials.
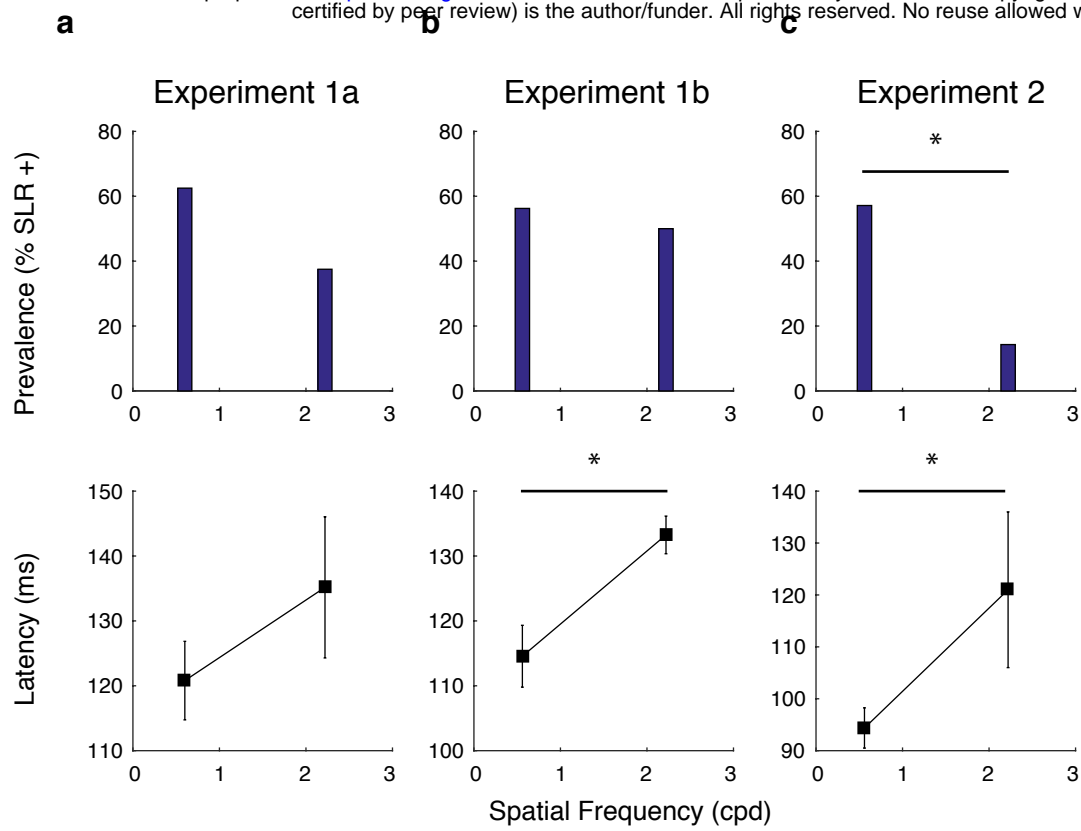
**Figure 7.** The influence of SF on SLR characteristics persisted for RT-matched trials. Same format as Fig. 5, using data matched for RT.
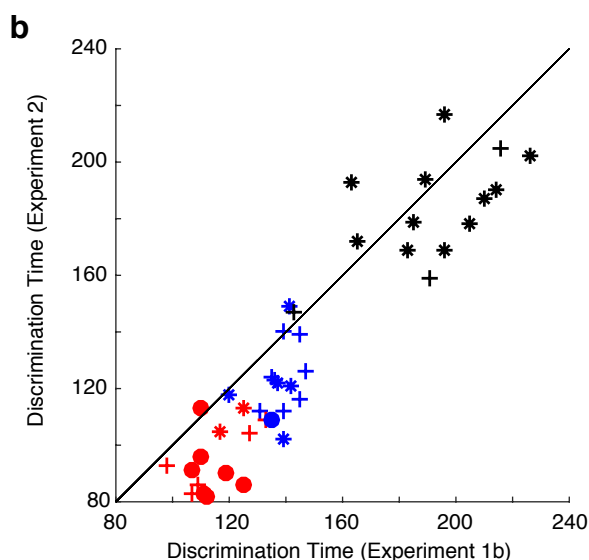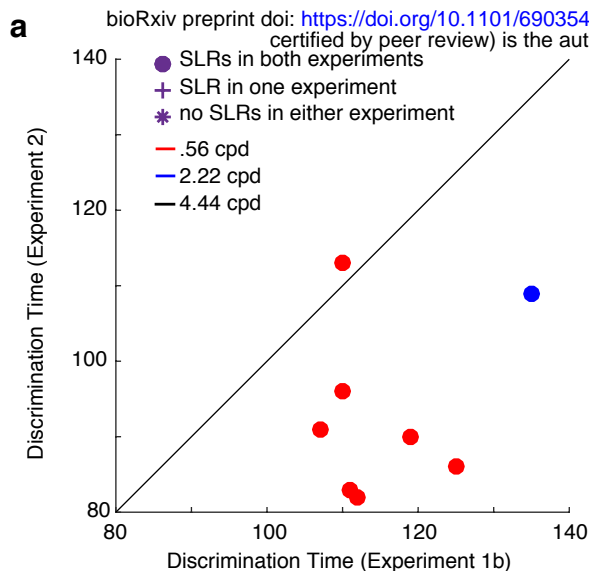
**Figure 8.** Discrimination times during on-line reach corrections (Experiment 2) plotted as a function of discrimination times for reaches initiated from a static posture (Experiment 1b). Discrimination times are derived from the time-series ROC analysis. Each data point depicts data from a unique combination of subject and stimulus SF (see colour scheme). (a) Data from occurrences with an SLR+ observation in both Experiments 1b and Experiment 2. (b) Data from all participants, with symbols depicting whether SLRs were observed in both experiments (dots, same data as in (a), but on a different time scale), whether an SLR was observed in only one experiment (crosses), or whether an SLR was not observed in either experiment (asterisks). Solid diagonal line shows line of unity. The clustering of data below the line of unity means that shorter discrimination times were observed in Experiment 2.
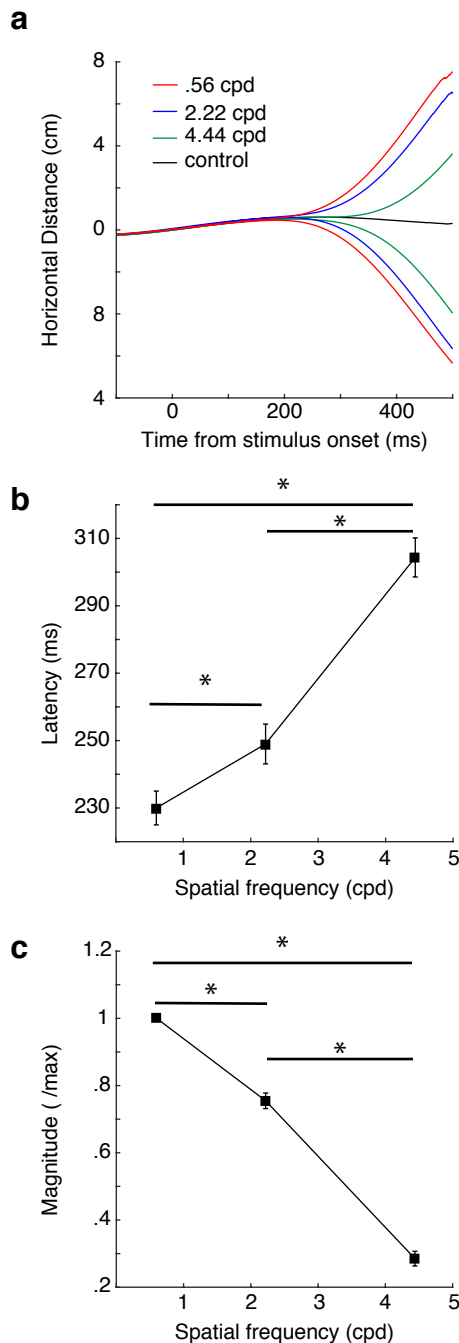
**a**



**b**



**c**



**Figure 9.** Characteristics of on-line reach corrections to different SFs in Experiment 2. (a) Results from a sample participant, depicting the mean lateral distance for on-line reach corrections to displaced stimuli composed of different SFs (coloured lines), or to the control condition where the reach target was not displaced (black line). (b, c) Latency (b) or magnitude (c) of on-line reach corrections across the sample, as a function of SF. The latency was derived from a time-series ROC analysis of lateral distance for left versus right displaced stimuli. The magnitude is normalized within each participant to the maximum correction. Error bars represent SEM.
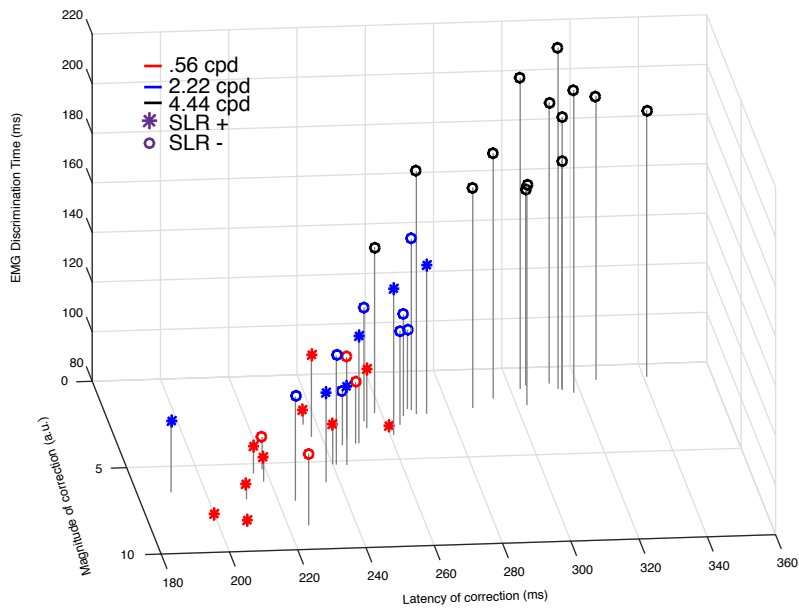
**Figure 10.** Three-way relationship between EMG discrimination, and the latency and magnitude of the on-line reach correction. Each point represents data from a single participant, colour-coded by SF, with the symbol indicating whether an SLR was observed (asterisks) or not (circles).